Reducing Redundancy in the Bottleneck Representation of the Autoencoders

Firas Laakom* , Jenni Raitoharju†, Alexandros Iosifidis‡ and Moncef Gabbouj*

*Department of Computing Sciences, Tampere University, Finland

†Programme for Environmental Information, Finnish Environment Institute, Finland

‡Department of Electrical and Computer Engineering, Aarhus University, Denmark

Emails: *firas.laakom@tuni.fi, †jenni.raitoharju@syke.fi, ‡ai@ece.au.dk, *moncef.gabbouj@tuni.fi

Abstract—Autoencoders are a type of unsupervised neural networks, which can be used to solve various tasks, e.g., dimensionality reduction, image compression, and image denoising. An AE has two goals: (i) compress the original input to a low-dimensional space at the bottleneck of the network topology using an encoder, (ii) reconstruct the input from the representation at the bottleneck using a decoder. Both encoder and decoder are optimized jointly by minimizing a distortion-based loss which implicitly forces the model to keep only those variations of input data that are required to reconstruct the and to reduce redundancies. In this paper, we propose a scheme to explicitly penalize feature redundancies in the bottleneck representation. To this end, we propose an additional loss term, based on the pair-wise correlation of the neurons, which complements the standard reconstruction loss forcing the encoder to learn a more diverse and richer representation of the input. We tested our approach across different tasks: dimensionality reduction using three different dataset, image compression using the MNIST dataset, and image denoising using fashion MNIST. The experimental results show that the proposed loss leads consistently to superior performance compared to the standard AE loss.

Index Terms—autoencoders, unsupervised learning, diversity, feature representation, dimensionality reduction, image denoising, image compression

I. INTRODUCTION

With the progress of data gathering techniques, high-dimensional data are available for training machine learning approaches. However, the impracticality of working in high dimensional spaces due to the *curse of dimensionality* and the understanding that the data in many problems reside on manifolds with much lower dimensions than those of the original space, has led to the development of various approaches which try to learn a mapping from the original space to a more meaningful lower-dimensional representation.

Autoencoders (AEs) [1] are a powerful data-driven unsupervised approach used to learn a compact representation of a given input distribution. An autoencoder focuses solely on finding a low dimensional representation, from which the input data can be reconstructed with minimal distortion. Autoencoders have been applied successfully in many applications, such as transfer learning [2], [3], [4], anomaly detection [5], [6], [7], [8], dimensionality reduction [9], [10], [11], and compression [12], [13], [14], [15].

The paper is under consideration at Pattern Recognition Letters

To accomplish these tasks, an autoencoder has two different parts: an encoder $g(\cdot)$, which maps an input $x \in \mathcal{X}$ to a compact low-dimensional space $g(x)$, called the bottleneck representation, and a decoder $f(\cdot)$, which takes the output of the encoder as its input and uses it to reconstruct the original input $f \circ g(x)$. Given a distortion metric $D \colon \mathcal{X} \times \mathcal{X} \to \mathbb{R}$, which measures the difference between the original input and the reconstructed input [16], [2], autoencoderss are trained in an end-to-end manner using gradient descent [1] to minimize the loss L defined as the average distortion over the training data $\{x_i\}_{i=1}^N$:

$$\min_{f,g} L\big(\{x_i\}_{i=1}^N\big) \triangleq \min_{f,g} \frac{1}{N} \sum_{i=1}^{N} D(x_i, f \circ g(x_i)). \quad (1)$$

Several extensions and regularization techniques have been proposed to augment this loss [2], [14], [12], [17], [18] to improve the performance of the model. The extension are able to improve the mapping of the inputs to compressed compact representations at the bottleneck of the autoencoder, so that the original inputs can be better reconstructed from these compact representations using the decoder.

By controlling the size of the bottleneck, one can explicitly control the dimensionality of the representation and the compression rate [19], [12]. However, a low size of the bottleneck increases the complexity of the task of the decoder risking a higher distortion rate. This trade-off forces the model to keep only those variations in the input data that are required to reconstruct the input and to avoid redundancies and noise within the input [16], [17]. This is achieved implicitly using back-propagation by minimizing the reconstruction error, i.e., distortion D.

In the context of supervised neural networks, it has been shown that reducing the correlation improves generalization [20], [21], [22]. Approaches helping to reduce the redundancy have been successfully applied, e.g., for network pruning [23], [24], [25], [26] and self-supervised learning [27]. In this paper, we propose to model the feature redundancy in the bottleneck representation and minimize it explicitly. To this end, we propose augmenting the distortion loss L using a redundancy loss computed as the sum of the pair-wise correlations between the elements of the bottleneck. The full schema is illustrated in Figure 1. We argue that explicitly penalizing the cross-covariance between the different units in
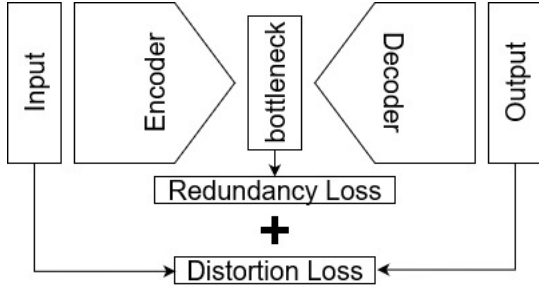
Fig. 1. An illustration on how the autoencoder loss is computed using our approach.

the bottleneck provides an extra feedback for the encoder to avoid redundancy and to learn a richer representation of the input samples.

The contributions of this paper can be summarized as follows:

- We propose a scheme to avoid redundant features in the bottleneck representation of autoencoders.
- We propose to augment the autoencoder loss to explicitly penalize the pair-wise correlations between the features and learn diverse compressed embedding of the samples.
- The proposed penalty acts as an unsupervised regularizer on top of the encoder and can be integrated into any autoencoder-based model in a plug-and-play manner.
- The proposed method is extensively evaluated over three tasks: dimensionality reduction, image compression, and image denoising. The results show a consistent performance boost compared to the standard approach.

The rest of this paper is organized as follows. Section II provides the background of autoencoders training strategies and a brief review of different applications considered in this work: dimensionality reduction, image compression, and image denoising. Section III presents the proposed approach. Section IV reports experimental results for dimensionality reduction task using three different datasets: Iris [28], Cancer Wisconsin [29], and the Digit [30] Datasets. Section V reports experimental results for the image compression task using the MNIST dataset [31]. Section VI evaluates our approach on the image denoising task using the fashionMNIST dataset [32]. Section VII concludes the paper.

II. RELATED WORK

Autoencoders were first introduced in [33] as a model trained to reconstruct its input, i.e., to approximate the identity function $f(x) \approx x$. While the identity function seems a particularly trivial function to learn, enforcing certain constraints on the network topology and particularly using a low number of units in the hidden representations [1] forces the model to learn to efficiently represent the data in a much lower-dimensional space compared to the original space [34]. This is a desired property in several applications, e.g., dimensionality reduction [9], [10], [11], compression [12], [13], [14], [15], and image denoising [35], [36], [37].

Dimensionality reduction refers to the problem of learning a mapping from a high-dimensional input space $\mathcal{X} \in \mathbb{R}^D$ into a lower-dimensional space $\mathcal{Z} \in \mathbb{R}^d$, where $d << D$, while preserving features of interest in the input data. Several linear [38], [39], [40] and non-linear [41], [42] approaches have been proposed to solve this task. Some are supervised approaches [43], [44], such as Linear Discriminant Analysis (LDA) [45], [46], [47] and Marginal Fisher Analysis (MFA) [48], others are unsupervised methods [49], [50], such as Principal Component Analysis (PCA) [51]. Dimensionality reduction is the most straightforward application of autoencoders [9], [10], [11]. The desired mapping can be learned using an autoencoder by setting the size of the bottleneck to d units and training the model to reconstruct a copy of the input.

Image compression is an important task in many applications. Recent advances in deep neural networks [1] have enabled efficient modeling of high-dimensional data and led to outperforming traditional compression techniques [52], [53], [54], [55], [56] in image compression [57], [58], [59]. Recently, there has been interest in autoencoders to solve this problem [60], [19], [17], [12], [61] due to their flexibility and easiness to train [12], [19], [62], [63].

Image denoising [64] refers to the problem of trying to restore a clean version of the image from its noisy corrupted counterpart. Due to their plug-and-play network architectures, CNN-based autoencoders have been widely adopted to solve this task [65], [66]. In particular, an autoencoder is trained using pairs of noisy and clean images. By taking the noisy sample as an input and setting the clean version as a target at the output end, the model learns to keep only the important information from the image and discard the noise.

III. REDUCING THE PAIR-WISE CORRELATION WITHIN THE BOTTLENECK REPRESENTATION

Autoencoders are a special type of neural networks trained to achieve two objectives: (i) to compress an input signal into a low-dimensional space, (ii) to reconstruct the original input from the low-dimensional representation. This is achieved by minimizing the reconstruction loss over the training samples, which implicitly forces a concise 'non-redundant' representation of the data. In this paper, we propose to augment the reconstruction loss to explicitly minimize the redundancy, i.e., correlation, between the features learned at the bottleneck.

Formally, given a training data $\{\boldsymbol{x}_i\}_{i=1}^N$ and an encoder $g(\cdot) \in \mathbb{R}^D$, the correlation between the ith and j^{th} features, g_i and g_j, can be expressed as follows:

$$C(g_i, g_j) = \frac{1}{N} \sum_n (g_i(\boldsymbol{x}_n) - \mu_i)(g_j(\boldsymbol{x}_n) - \mu_j), \quad (2)$$

where $\mu_i = \frac{1}{N} \sum_n g_i(\boldsymbol{x}_n)$ is the average output of the ith neuron. Our aim is to minimize the redundancy of the bottleneck representations which corresponds to minimizing the pair-wise covariance between different features. Thus, we

TABLE I
STATISTICS OF THE THREE DATASET

Dataset	Dimensionality	# Classes	Samples per class
IRIS [28]	4	3	50
Wisconsin [29]	30	2	212-357
Digits [30]	64	10	∼180

TABLE II
AVERAGE AND STANDARD DEVIATION OF RMSE OF DIFFERENT
APPROACHES ON THREE DIFFERENT DATASETS OVER 5 REPETITIONS

	Iris	Wisconsin	Digits
standard	0.0873 ± 0.0438	0.0717 ± 0.0056	0.1876 ± 0.0049
ours (0.1)	**0.0584 ± 0.0038**	0.0704 ± 0.0047	**0.1826 ± 0.0028**
ours (0.05)	0.0609 ± 0.0090	0.0712 ± 0.0048	0.1844 ± 0.0051
ours (0.01)	0.0656 ± 0.0154	0.0690 ± 0.0062	0.1842 ± 0.0076
ours (0.005)	**0.0584 ± 0.0028**	**0.0683 ± 0.0055**	0.1874 ± 0.0093
ours (0.001)	0.0795 ± 0.0466	0.0688 ± 0.0053	0.1859 ± 0.0037

augment the standard loss $L\big(\{\boldsymbol{x}_i\}_{i=1}^N\big)$ as follows:

$$L\big(\{\boldsymbol{x}_i\}_{i=1}^N\big)_{aug} \triangleq L\big(\{\boldsymbol{x}_i\}_{i=1}^N\big) + \alpha \sum_{i \neq j} C(g_i, g_j)$$

$$= \frac{1}{N} \sum_{i=1}^N D(\boldsymbol{x}_i, f \circ g(\boldsymbol{x}_i)) \qquad (3)$$

$$+ \alpha \sum_{i \neq j} \Big(\frac{1}{N} \sum_n (g_i(\boldsymbol{x}_n) - \mu_i)(g_j(\boldsymbol{x}_n) - \mu_j) \Big),$$

$$(4)$$

where α is a hyper-parameter used to control the contribution of the additional term in the total loss of the model. L_{aug} is composed of two terms, the first term is the traditional autoencoder loss that depends on both the encoder and decoder parts to ensure that the autoencoder learns to reconstruct the input, while the second term depends only on the encoder and its aim is to promote the diversity of the learned features and to ensure that the encoder learns less correlated non-redundant features.

Intuitively, the proposed approach acts as an unsupervised regularizer on top of the encoder providing an extra feedback during the back-propagation to reduce the correlations of the encoder's output. The proposed scheme can be embedded into any autoencoder-based model as a plug-in and optimized in a batch-manner, i.e., at each optimization step, we can compute the covariance using the batch samples. Moreover, it is suitable for different learning strategies and different topologies.

IV. EXPERIMENTS ON DIMENSIONALITY REDUCTION

In this section, we consider the problem of dimensionality reduction using an autoencoder. We test the proposed approach using three different tabular dataset: Iris [28], Cancer Wisconsin [29], and the Digits [30]. The important statistics of three datasets are summarized in Table I. The Iris dataset [28] contains samples from three different Iris flower categories. Each sample is represented in a four-dimensional space and there is a total of 50×3 samples. The Cancer Wisconsin dataset [29] is composed of 569 samples with features computed from a digitized image of a fine needle aspirate of a breast mass. These features describe characteristics of the cell nuclei present in the image. The Digits dataset [30] is composed of 1797 8×8 pixel images of digits. Each image sample is of a hand-written digit and its features are represented with a 64-dimensional vector.

As the autoencoder topology, we use a simple architecture, where the encoder maps the input using two intermediate fully-connected layers composed of 10 units with ReLU activation. Then, the bottleneck representation of size d is obtained using a fully-connected layer with d units and Leaky ReLU [67] activation. Symmetrically, the decoder is composed of

two 10-dimensional fully-connected layers followed by ReLU activation and an output layer with the same size as the input using a sigmoid activation. The value of d is set to 2 for Iris and 6 for both Wisconsin and the Digit datasets. For training, we use Adam as our optimizer with a learning rate of 1×10^{-2} and the mean square error loss as our standard training loss L. The number of epochs and the batch size are set to 100 and 32 in in all experiments, respectively. For all experiments, we use 75% of the data for the training and the remaining 25% for testing. Each experiment is repeated 5 times and the mean and standard deviation of the root mean square error (RMSE) on the test set are reported.

In Table II, we report the experimental results using the standard loss and our proposed augmented loss using different values of hyper-parameter α, introduced in equation 4, in the range $\{0.1, 0.05, 0.01, 0.005, 0.001\}$. It can be seen in the table that, by explicitly penalizing the redundancy in the bottleneck representation, our approach consistently achieves lower rates compared to the standard approach on the three datasets.

For the Iris dataset, the best performance is achieved using our approach with an α equal to 0.1 or 0.005, which improves the results on average $\sim 33\%$ compared to the standard approach. For the Wisconsin dataset, using our approach with the hyperparameter α set to 0.005 achieves a 4.7% average improvement compared to the standard approach, whereas, for the Digit dataset, the best performance is achieved using $\alpha = 0.1$.

V. EXPERIMENTS ON IMAGE COMPRESSION

In this section, we consider the problem of image compression using an autoencoder. We test the proposed approach using the MNIST dataset [31], which is a handwritten digit dataset composed of 10 classes. MNIST images are 28×28 pixels, which results in 784-dimensional vectors. The dataset has 50000 samples for training and 10000 for testing.

For the autoencoder model, we use a simple architecture. The encoder is composed of two intermediate fully-connected layers composed of 256 and 128 units, respectively. The final output of the encoder is composed of d units, where d is the size of the bottleneck. Similarly, the decoder part takes the encoder's output, maps it to an intermediate layer of 128 units, then 256 units, and outputs a 784-vector. In all the layers, we use ReLU activation except for the final output, where sigmoid activation is used.

For the training, we use Adam as our optimizer with a learning rate of 1×10^{-2} and the mean square loss as our standard training loss L. We train with 80% of the original

TABLE III
AVERAGE AND STANDARD DEVIATION OF RMSE, PSNR, AND SSIM OF
DIFFERENT APPROACHES ON THE MNIST DATASET OVER 5 REPETITIONS

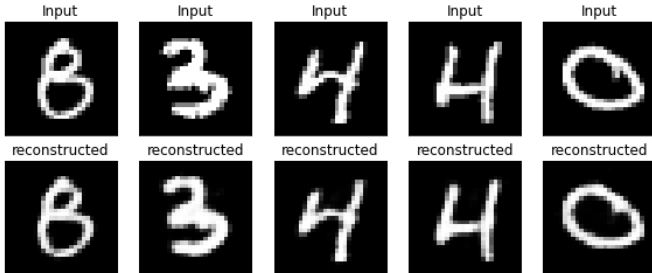|	RMSE ↓	PSNR ↑	SSIM ↑
	784 → 256		
Standard	0.0518 ± 0.0005	0.9631 ± 0.0016	26.43 ± 0.09
ours(0.1)	0.0508 ± 0.0005	0.9641 ± 0.0010	26.57 ± 0.11
ours(0.05)	0.0508 ± 0.0005	0.9636 ± 0.0007	26.58 ± 0.08
ours(0.01)	0.0513 ± 0.0005	**0.9647 ± 0.0013**	26.49 ± 0.09
ours(0.005)	**0.0506 ± 0.0007**	0.9635 ± 0.0012	**26.61 ± 0.10**
	784 → 64		
Standard	0.0596 ± 0.0021	0.9597 ± 0.0022	25.25 ± 0.29
Ours(0.1)	**0.0584 ± 0.0010**	**0.9607 ± 0.0012**	**25.42 ± 0.16**
Ours(0.05)	0.0588 ± 0.0018	0.9604 ± 0.0017	25.38 ± 0.25
Ours(0.01)	0.0593 ± 0.0010	0.9599 ± 0.0012	25.30 ± 0.15
Ours(0.005)	0.0588 ± 0.0009	0.9602 ± 0.0013	25.35 ± 0.13

Fig. 2. An illustration of the performance of our approach on image compression. First row contains the original inputs and the second row contains their reconstructed versions using our approach.

TABLE IV
AVERAGE AND STANDARD DEVIATION OF RMSE, PSNR, AND SSMI
SCORES OF DIFFERENT APPROACHES ON THE FASHIONMNIST DATASET
OVER 5 REPETITIONS WITH DIFFERENT NOISE RATES

	RMSE ↓	PSNR ↑	SSIM ↑
	$\beta = 0.1$		
Standard	0.0796 ± 0.0016	0.7980 ± 0.0061	22.51 ± 0.19
Ours (0.1)	0.0786 ± 0.0009	0.8018 ± 0.0024	22.64 ± 0.13
Ours (0.05)	**0.0772 ± 0.0018**	0.8049 ± 0.0062	**22.84 ± 0.25**
Ours (0.01)	0.0779 ± 0.0019	0.8047 ± 0.0066	22.77 ± 0.27
Ours (0.005)	0.0774 ± 0.0012	**0.8058 ± 0.0044**	22.82 ± 0.18
	$\beta = 0.2$		
Standard	0.0941 ± 0.0026	0.7283 ± 0.0110	20.95 ± 0.25
Ours (0.1)	0.0934 ± 0.0021	0.7301 ± 0.0102	21.03 ± 0.19
Ours (0.05)	0.0933 ± 0.0020	0.7290 ± 0.0079	21.04 ± 0.19
Ours (0.01)	0.0975 ± 0.0034	0.7143 ± 0.1276	20.63 ± 0.31
Ours (0.005)	**0.0922 ± 0.0012**	**0.7357 ± 0.0058**	**21.14 ± 0.13**
	$\beta = 0.4$		
Standard	0.1262 ± 0.0021	0.5901 ± 0.0089	18.27 ± 0.16
Ours (0.1)	**0.1258 ± 0.0021**	**0.5954 ± 0.0095**	**18.30 ± 0.15**
Ours (0.05)	0.1260 ± 0.0016	0.5946 ± 0.0067	18.28 ± 0.12
Ours (0.01)	0.1266 ± 0.0014	0.5865 ± 0.0070	18.22 ± 0.09
Ours (0.005)	0.1260 ± 0.0017	0.5911 ± 0.0085	18.28 ± 0.13

10,000 test samples. To construct a noisy dataset, we add a random noise from normal distribution $\beta \times \mathcal{N}(0, 1)$, where β is a hyperparameter controlling the noise rate. In Figure 3, we illustrate how the training samples are constructed from the original samples by adding the noise.
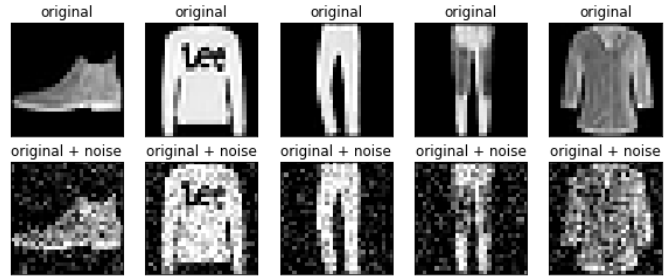

Fig. 3. An illustration of how the noise is added to 5 samples from fashionMNIST dataset with $\beta = 0.2$. First row contains the original samples and second row contains there corresponding noisy samples.

training data and hold the remaining 20% as a validation set. During the training, the model with the lowest mean square error on the validation set is saved and used in the testing phase. We repeat each experiment five times and report the mean and standard deviation of the oot-mean-square error (RMSE) errors, the Peak signal-to-noise ratio (PSNR), and structural index similarity (SSIM) scores on the test set for the different approaches. We experiment with two different bottleneck sizes, i.e., 256 and 64. The results for different bottleneck sizes are reported in Table III.

We note that the proposed approach consistently boosts the performance of the autoencoder and yields lower RMSE errors compared to training with the standard loss only and higher PSNR and SSMI scores. For $d = 256$, the lowest RMSE score is achieved using the rate of 0.005 and the highest PSNR and SSMI scores are obtained by setting α to 0.01 and 0.005, respectively. For $d = 64$, α equal to 0.1 corresponds to the best scores across all the metrics. Figure 2 presents visual outputs of images reconstructed from the feature representation learned by our approach for $d = 64$. We note that our approach is able to learn to compress and reconstruct the input without any major distortion to the input.

VI. EXPERIMENTS ON IMAGE DENOISING

In this section, we consider the problem of image denoising using an autoencoder. We test the proposed approach using the fashionMNIST dataset [32], which is an image dataset composed of 10 classes. Each sample is a 28×28 gray-scale image. The dataset has a total of 60,000 training samples and

As the autoencoder model, we use a simple CNN-based architecture. The encoder is composed of two convolutional layer 3×3 filters with sizes 16 and 4, respectively. Symmetrically, the decoder is composed of two transposed convolutional layers of sizes 4 and 16 and a final convolutional layer with one filter with kernel size 3×3. All the layers have ReLU activation function except for the last layer where we use sigmoid activation. Each model is trained for 50 epochs using the mean square error loss and Adam optimizer. We repeat each experiment five times and report the means and standard deviations of RMSE, PSNR, and SSMI scores for different noise rates.

In Table IV, we report the experimental results for three different noise rates β: 0.1, 0.2, and 0.4. Except for the hyperparameter $\alpha = 0.01$ with noise rates 0.2 and 0.4, we note that our approach by explicitly minimizing the redundancy in the feature space constantly outperforms the standard approach accross all metrics. For the noise rate $\beta = 0.1$, the lowest RMSE rate and the highest SSMI score are achieved using our
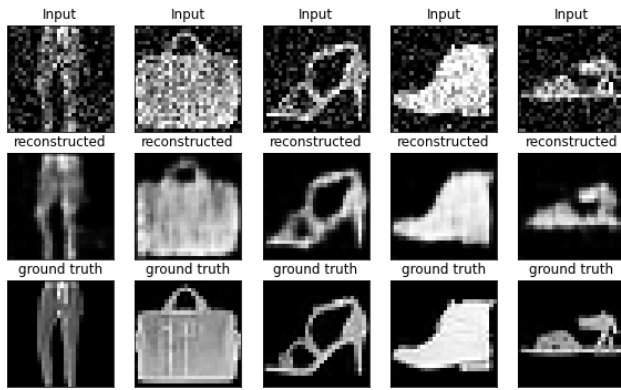
Fig. 4. Visual illustration of the performance of our approach on Image denoising. The first raw contains 5 input samples. Second raw and third raw present the output of our approach and the ground truth, respectively.

approach with α equal to 0.05, while the top PSNR is achieved with rates 0.005, whereas for a noise rate of 0.2, the best scores across all metrics correspond to $\alpha = 0.005$. For the extreme noise case, i.e., $\beta = 0.4$, our approach with $\alpha = 0.1$ achieves the best performance across the three metrics. In Figure 4, we present visual outputs for our approach. As shown, our approach learns to efficiently discard the noise from the input images.

VII. CONCLUSION

In this paper, we proposed a schema for modeling the redundancies at the bottleneck of an autoencoder. We proposed to complement the loss with an extra regularizer, which explicitly penalizes the pair-wise correlation of the neurons at the encoder's output and, thus, forces it to learn more diverse and compact representations for the input samples. The proposed approach can be interpreted as an unsupervised regularizer on top of the encoder and can be integrated into any autoencoder-based model in a plug-and-play manner. We empirically demonstrated the effectiveness of our approach across multiple tasks, dimensionality reduction, compression, and denoising ,and we showed that it boosts the performance compared to the standard approach. Future directions include extensive testing of our approach with deep autoencoders and proposing more efficient redundancy modeling techniques to improve the performance of autoencoders.

ACKNOWLEDGMENT

REFERENCES

[1] I. Goodfellow, Y. Bengio, A. Courville, and Y. Bengio, *Deep learning*. MIT Press, 2016, vol. 1.

[2] J. Deng, Z. Zhang, E. Marchi, and B. Schuller, "Sparse autoencoder-based feature transfer learning for speech emotion recognition," in *2013 humaine association conference on affective computing and intelligent interaction*. IEEE, 2013, pp. 511–516.

[3] F. Zhuang, X. Cheng, P. Luo, S. J. Pan, and Q. He, "Supervised representation learning: Transfer learning with deep autoencoders," in *Twenty-Fourth International Joint Conference on Artificial Intelligence*, 2015.

[4] C. Kandaswamy, L. M. Silva, L. A. Alexandre, R. Sousa, J. M. Santos, and J. M. de Sá, "Improving transfer learning accuracy by reusing stacked denoising autoencoders," in *2014 IEEE International Conference on Systems, Man, and Cybernetics (SMC)*. IEEE, 2014, pp. 1380–1387.

[5] L. Beggel, M. Pfeiffer, and B. Bischl, "Robust anomaly detection in images using adversarial autoencoders," in *Joint European Conference on Machine Learning and Knowledge Discovery in Databases*. Springer, 2019, pp. 206–222.

[6] Y. Zhao, B. Deng, C. Shen, Y. Liu, H. Lu, and X.-S. Hua, "Spatio-temporal autoencoder for video anomaly detection," in *Proceedings of the 25th ACM international conference on Multimedia*, 2017, pp. 1933–1941.

[7] R. C. Aygun and A. G. Yavuz, "Network anomaly detection with stochastically improved autoencoder based models," in *2017 IEEE 4th International Conference on Cyber Security and Cloud Computing (CSCloud)*. IEEE, 2017, pp. 193–198.

[8] C. Zhou and R. C. Paffenroth, "Anomaly detection with robust deep autoencoders," in *Proceedings of the 23rd ACM SIGKDD international conference on knowledge discovery and data mining*, 2017, pp. 665–674.

[9] S. Petscharnig, M. Lux, and S. Chatzichristofis, "Dimensionality reduction for image features using deep learning and autoencoders," in *Proceedings of the 15th international workshop on content-based multimedia indexing*, 2017, pp. 1–6.

[10] S. A. Thomas, A. M. Race, R. T. Steven, I. S. Gilmore, and J. Bunch, "Dimensionality reduction of mass spectrometry imaging data using autoencoders," in *2016 IEEE Symposium Series on Computational Intelligence (SSCI)*. IEEE, 2016, pp. 1–7.

[11] W. Wang, Y. Huang, Y. Wang, and L. Wang, "Generalized autoencoder: A neural network framework for dimensionality reduction," in *Proceedings of the IEEE conference on computer vision and pattern recognition workshops*, 2014, pp. 490–497.

[12] L. Theis, W. Shi, A. Cunningham, and F. Huszár, "Lossy image compression with compressive autoencoders," *arXiv preprint arXiv:1703.00395*, 2017.

[13] J. Han, S. Lombardo, C. Schroers, and S. Mandt, "Deep generative video compression," *arXiv preprint arXiv:1810.02845*, 2018.

[14] A. Golinski, R. Pourreza, Y. Yang, G. Sautiere, and T. S. Cohen, "Feedback recurrent autoencoder for video compression," in *Proceedings of the Asian Conference on Computer Vision*, 2020.

[15] L. Yingzhen and S. Mandt, "Disentangled sequential autoencoder," in *International Conference on Machine Learning*. PMLR, 2018, pp. 5670–5679.

[16] P. Baldi, "Autoencoders, unsupervised learning, and deep architectures," in *Proceedings of ICML Workshop on Unsupervised and Transfer Learning*, vol. 27, 02 Jul 2012, pp. 37–49.

[17] Z. Cheng, H. Sun, M. Takeuchi, and J. Katto, "Deep convolutional autoencoder-based lossy image compression," in *2018 Picture Coding Symposium (PCS)*. IEEE, 2018, pp. 253–257.

[18] B. Seybold, E. Fertig, A. Alemi, and I. Fischer, "Dueling decoders: Regularizing variational autoencoder latent spaces," *arXiv preprint arXiv:1905.07478*, 2019.

[19] Y. Hu, W. Yang, Z. Ma, and J. Liu, "Learning end-to-end lossy image compression: A benchmark," *arXiv preprint arXiv:2002.03711*, 2020.

[20] F. Laakom, J. Raitoharju, A. Iosifidis, and M. Gabbouj, "Within-layer diversity reduces generalization gap," *arXiv preprint arXiv:2106.06012*, 2021.

[21] M. Cogswell, F. Ahmed, R. B. Girshick, L. Zitnick, and D. Batra, "Reducing overfitting in deep networks by decorrelating representations," in *International Conference on Learning Representations*, 2016.

[22] F. Laakom, J. Raitoharju, A. Iosifidis, and M. Gabbouj, "On feature diversity in energy-based models," in *Energy Based Models Workshop-ICLR 2021*, 2021.

[23] Y. Kondo and K. Yamauchi, "A dynamic pruning strategy for incremental learning on a budget," in *International Conference on Neural Information Processing*. Springer, 2014, pp. 295–303.

[24] Y. He, P. Liu, Z. Wang, Z. Hu, and Y. Yang, "Filter pruning via geometric median for deep convolutional neural networks acceleration," in *Proceedings of the IEEE Conference on Computer Vision and Pattern Recognition*, 2019, pp. 4340–4349.

[25] P. Singh, V. K. Verma, P. Rai, and V. Namboodiri, "Leveraging filter correlations for deep model compression," in *The IEEE Winter Conference on Applications of Computer Vision*, 2020, pp. 835–844.

[26] S. Lee, B. Heo, J.-W. Ha, and B. C. Song, "Filter pruning and re-initialization via latent space clustering," *IEEE Access*, vol. 8, pp. 189 587–189 597, 2020.

[27] J. Zbontar, L. Jing, I. Misra, Y. LeCun, and S. Deny, "Barlow twins: Self-supervised learning via redundancy reduction," *arXiv preprint arXiv:2103.03230*, 2021.

[28] R. A. Fisher, "The use of multiple measurements in taxonomic problems," *Annals of eugenics*, vol. 7, no. 2, pp. 179–188, 1936.

[29] W. N. Street, W. H. Wolberg, and O. L. Mangasarian, "Nuclear feature extraction for breast tumor diagnosis," in *Biomedical image processing and biomedical visualization*, vol. 1905. International Society for Optics and Photonics, 1993, pp. 861–870.

[30] F. Alimoglu and E. Alpaydin, "Methods of combining multiple classifiers based on different representations for pen-based handwritten digit recognition," in *Proceedings of the Fifth Turkish Artificial Intelligence and Artificial Neural Networks Symposium (TAINN 96.* Citeseer, 1996.

[31] Y. LeCun, L. Bottou, Y. Bengio, and P. Haffner, "Gradient-based learning applied to document recognition," *Proceedings of the IEEE*, vol. 86, no. 11, pp. 2278–2324, 1998.

[32] H. Xiao, K. Rasul, and R. Vollgraf, "Fashion-mnist: a novel image dataset for benchmarking machine learning algorithms," *arXiv preprint arXiv:1708.07747*, 2017.

[33] D. E. Rumelhart, G. E. Hinton, and R. J. Williams, "Learning internal representations by error propagation," California Univ San Diego La Jolla Inst for Cognitive Science, Tech. Rep., 1985.

[34] P. Baldi, "Autoencoders, unsupervised learning, and deep architectures," in *Proceedings of ICML workshop on unsupervised and transfer learning.* JMLR Workshop and Conference Proceedings, 2012, pp. 37–49.

[35] X. Ye, L. Wang, H. Xing, and L. Huang, "Denoising hybrid noises in image with stacked autoencoder," in *2015 IEEE International Conference on Information and Automation.* IEEE, 2015, pp. 2720–2724.

[36] P. Vincent, H. Larochelle, Y. Bengio, and P.-A. Manzagol, "Extracting and composing robust features with denoising autoencoders," in *Proceedings of the 25th international conference on Machine learning*, 2008, pp. 1096–1103.

[37] L. Gondara, "Medical image denoising using convolutional denoising autoencoders," in *2016 IEEE 16th International Conference on Data Mining Workshops (ICDMW).* IEEE, 2016, pp. 241–246.

[38] W. Zhao, R. Chellappa, and P. J. Phillips, *Subspace linear discriminant analysis for face recognition.* Citeseer, 1999.

[39] Y. Koren and L. Carmel, "Robust linear dimensionality reduction," *IEEE transactions on visualization and computer graphics*, vol. 10, no. 4, pp. 459–470, 2004.

[40] F. Laakom, J. Raitoharju, N. Passalis, A. Iosifidis, and M. Gabbouj, "Graph embedding with data uncertainty," *arXiv preprint arXiv:2009.00505*, 2020.

[41] D. DeMers and G. W. Cottrell, "Non-linear dimensionality reduction," in *Advances in neural information processing systems.* Citeseer, 1993, pp. 580–587.

[42] Y.-R. Yeh, S.-Y. Huang, and Y.-J. Lee, "Nonlinear dimension reduction with kernel sliced inverse regression," *IEEE transactions on Knowledge and Data Engineering*, vol. 21, no. 11, pp. 1590–1603, 2008.

[43] Y. Liu, R. Zhang, F. Nie, X. Li, and C. Ding, "Supervised dimensionality reduction methods via recursive regression," *IEEE Transactions on Neural Networks and Learning Systems*, 2019.

[44] M. Sugiyama, "Local fisher discriminant analysis for supervised dimensionality reduction," in *Proceedings of the 23rd international conference on Machine learning*, 2006, pp. 905–912.

[45] S. Balakrishnama and A. Ganapathiraju, "Linear discriminant analysis-a brief tutorial," *Institute for Signal and information Processing*, vol. 18, no. 1998, pp. 1–8, 1998.

[46] C. Li, Y. Shao, W. Yin, and M. Liu, "Robust and sparse linear discriminant analysis via an alternating direction method of multipliers," *IEEE Transactions on Neural Networks and Learning Systems*, 2020.

[47] A. Iosifidis, A. Tefas, and I. Pitas, "On the optimal class representation in linear discriminant analysis," *IEEE Transactions on Neural Networks and Learning Systems*, 2013.

[48] S. Yan, D. Xu, B. Zhang, H.-J. Zhang, Q. Yang, and S. Lin, "Graph embedding and extensions: A general framework for dimensionality reduction," *IEEE Transactions on Pattern Analysis and Machine Intelligence*, no. 1, pp. 40–51, 2007.

[49] A. C. Kumar, "Analysis of unsupervised dimensionality reduction techniques," *Computer science and information systems*, vol. 6, no. 2, pp. 217–227, 2009.

[50] M. Dash, H. Liu, and J. Yao, "Dimensionality reduction of unsupervised data," in *Proceedings ninth ieee international conference on tools with artificial intelligence.* IEEE, 1997, pp. 532–539.

[51] S. Wold, K. Esbensen, and P. Geladi, "Principal component analysis," *Chemometrics and intelligent laboratory systems*, vol. 2, no. 1-3, pp. 37–52, 1987.

[52] K. Ullrich, E. Meeds, and M. Welling, "Soft weight-sharing for neural network compression," *arXiv preprint arXiv:1702.04008*, 2017.

[53] F. Mentzer, L. V. Gool, and M. Tschannen, "Learning better lossless compression using lossy compression," in *Proceedings of the IEEE/CVF Conference on Computer Vision and Pattern Recognition*, 2020, pp. 6638–6647.

[54] M. W. Marcellin, M. J. Gormish, A. Bilgin, and M. P. Boliek, "An overview of jpeg-2000," in *Proceedings DCC 2000. Data Compression Conference.* IEEE, 2000, pp. 523–541.

[55] A. Skodras, C. Christopoulos, and T. Ebrahimi, "The jpeg 2000 still image compression standard," *IEEE Signal processing magazine*, vol. 18, no. 5, pp. 36–58, 2001.

[56] M. Rabbani and P. W. Jones, *Digital image compression techniques.* SPIE press, 1991, vol. 7.

[57] K. Gregor, F. Besse, D. J. Rezende, I. Danihelka, and D. Wierstra, "Towards conceptual compression," *arXiv preprint arXiv:1604.08772*, 2016.

[58] G. Toderici, D. Vincent, N. Johnston, S. Jin Hwang, D. Minnen, J. Shor, and M. Covell, "Full resolution image compression with recurrent neural networks," in *Proceedings of the IEEE Conference on Computer Vision and Pattern Recognition*, 2017, pp. 5306–5314.

[59] J. Ballé, V. Laparra, and E. P. Simoncelli, "End-to-end optimization of nonlinear transform codes for perceptual quality," in *2016 Picture Coding Symposium (PCS).* IEEE, 2016, pp. 1–5.

[60] Y. Ollivier, "Auto-encoders: reconstruction versus compression," *arXiv preprint arXiv:1403.7752*, 2014.

[61] O. Rippel and L. Bourdev, "Real-time adaptive image compression," in *International Conference on Machine Learning.* PMLR, 2017, pp. 2922–2930.

[62] F. Jiang, W. Tao, S. Liu, J. Ren, X. Guo, and D. Zhao, "An end-to-end compression framework based on convolutional neural networks," *IEEE Transactions on Circuits and Systems for Video Technology*, vol. 28, no. 10, pp. 3007–3018, 2017.

[63] Y. Yang, R. Bamler, and S. Mandt, "Improving inference for neural image compression," *arXiv preprint arXiv:2006.04240*, 2020.

[64] K. Gupta and S. Gupta, "Image denoising techniques-a review paper," *IJITEE*, vol. 2, pp. 6–9, 2013.

[65] C. Tian, L. Fei, W. Zheng, Y. Xu, W. Zuo, and C.-W. Lin, "Deep learning on image denoising: An overview," *Neural Networks*, 2020.

[66] B. Goyal, A. Dogra, S. Agrawal, B. Sohi, and A. Sharma, "Image denoising review: From classical to state-of-the-art approaches," *Information fusion*, vol. 55, pp. 220–244, 2020.

[67] A. L. Maas, A. Y. Hannun, and A. Y. Ng, "Rectifier nonlinearities improve neural network acoustic models," in *International Conference on Machine Learning.* Citeseer, 2013.